GMR
The Original

THYMOQUINONE TREATMENT ALTERS CELL CYCLE DISTRIBUTION IN PA-1 OVARIAN CANCER CELLS: A FLOW CYTOMETRIC ANALYSIS

Subhashini Y[1], Dr. Sasi Kumar[2*], Dr. S. Subamalani[3], Dr. G Raghuramaiah[4],Dr. J C Swarnalatha[5]

[1]Ph.D Scholar, Meenakshi Academy of Higher education and Research, Chennai, Tamil Nadu.
[*2]Professor, Department of Physiology, VELS Medical College and Hospital, Manjankaranai, Tamil Nadu.
[3]Professor, Department of Physiology, Tagore Medical College and Hospital, Chennai, Tamil Nadu.
[4] Assistant professor, Department of Anatomy, Malla Reddy Medical College for Women, Hyderabad, Telangana
[5]Assistant Professor, Department of Biochemistry, Government Medical College & GGH, Mahabubnagar, Telangana.
*Corresponding Author: Dr. Sasi Kumar, simmamsasi@gmail.com

ABSTRACT

Background: Ovarian cancer has the highest mortality rate among gynecological cancers. Thymoquinone, extracted from Nigella sativa, exhibits anticancer activity in multiple experimental models; however, its effects on ovarian cancer cell cycle dynamics have not been systematically characterized.

Objective: We examined redistribution of cell cycle phases and cytotoxicity following thymoquinone exposure in PA-1 ovarian cancer cells.

Methods: PA-1 cells were treated with thymoquinone or vehicle control. Flow cytometry was used to quantify the G1, S, and G2 phase distributions (n=3 technical replicates per group). The MTT assay was used to assess viability across the 0–100 µg/mL thymoquinone concentration range. We applied Welch's t-test with a Benjamini-Hochberg false-discovery rate adjustment for between-group comparisons.

Results: Thymoquinone shifted the cell cycle distribution across all measured phases. G1 increased from 42.35±1.88% to 53.91±1.43%, a 27% relative increase (FDR-adjusted p=0.00317). S phase declined from 20.64±1.00% to 15.53±0.82% (p=0.00509), a 25% reduction. G2 decreased from 35.93±2.37% to 28.94±0.27% (p=0.0425), a 19% reduction. All three phase changes survived multiple-comparison corrections. Viability declined with increasing concentration, producing an IC50 of 78.77 µg/mL.

Conclusion: Thymoquinone treatment enriched the G1 phase cells in PA-1 ovarian cancer while depleting the S and G2 phases. This redistribution pattern indicates interference at the G1/S checkpoint and supports investigation of thymoquinone as a cell-cycle-modulating agent in ovarian cancer.

KEYWORDS: thymoquinone, ovarian cancer, PA-1 cells, cell cycle arrest, G1 phase, flow cytometry, cytotoxicity

INTRODUCTION

Ovarian cancer accounts for approximately 5% of cancer-related deaths in women and has the highest mortality rate among gynecological malignancies (1). Five-year survival rates for advanced-stage disease remain below 30%, despite advances in surgical and chemotherapeutic approaches (2). The emergence of platinum resistance and dose-limiting toxicities necessitates the development of novel therapeutic strategies (3).

Natural compounds are a promising source of anticancer agents (4). Thymoquinone (2-isopropyl-5-methylbenzo-1,4-quinone), the principal bioactive component of Nigella sativa seed oil, exhibits anticancer activity in breast, colon, and lung cancer models (5,6). Proposed mechanisms include cell cycle modulation, induction of apoptosis, and generation of oxidative stress (7,8).

Cell cycle dysregulation is a hallmark of cancer (9). The G1/S transition checkpoint regulates cellular proliferation (10). Previous studies have reported the effects of thymoquinone on the cell cycle in various cancer cell lines; however, flow cytometric analysis in ovarian cancer models remains limited (11, 12).

The PA-1 cell line, which originates from a human ovarian teratocarcinoma, is commonly used in ovarian cancer research (13). This study characterized the effect of thymoquinone on cell-cycle distribution in PA-1 cells using flow cytometry and assessed cell viability using the MTT assay.

MATERIALS AND METHODS

Data Sources

This analysis used flow cytometry data from PA-1 human ovarian cancer cells treated with thymoquinone or a vehicle control. Cell cycle analysis data were obtained from flow_results_long_standard.csv, which contains the percentages of cells in the G1, S, and G2 phases for three technical replicates per experimental group (control and treatment).

We obtained cell-cycle data from flow cytometry experiments on PA-1 human ovarian cancer cells treated with thymoquinone or vehicle control. Each group included three technical replicates. We extracted the cell cycle phase

percentages (G1, S, and G2) for individual replicates from flow_results_long_standard.csv. Summary statistics (mean, standard deviation, and p-values) were obtained from flow_stats_summary.csv (14). The quality control metrics were obtained from qc_sums.csv. MTT viability data across 11 thymoquinone concentrations (0–100 µg/mL) were obtained from mtt_viability_table.csv.

Quality Control
Flow cytometry data quality was verified by confirming that the sum of all cell cycle phase percentages approximated 100% across replicates. All replicates met this criterion, with phase sums ranging from 97.62% to 100.08%.

Statistical Analysis
Cell cycle data are presented as mean ± standard deviation from three technical replicates per group for each treatment. Between-group comparisons for each cell cycle phase were performed using Welch's two-sample t-test. To control for multiple comparisons across the three cell cycle phases, p-values were adjusted using the Benjamini-Hochberg false discovery rate (FDR) procedure. Statistical significance was defined as an FDR-adjusted p-value of <0.05.

IC50 Determination
The half-maximal inhibitory concentration (IC50) of thymoquinone was estimated from MTT viability data by linear interpolation between two concentrations bracketing 50% viability.

RESULTS

Dataset Overview
Cell cycle analysis included control and thymoquinone-treated PA-1 cells, with three technical replicates per group (Table 1). All replicates passed the quality control. The MTT viability assay included 11 concentrations ranging from 0 to 100 µg/mL.

Table 1: Dataset Overview

Component	Role in manuscript	Groups/conditions	Replicates per group	Measurements reported	Units
Cell cycle dataset	Primary endpoint	Control, Treated	3	G1, S, G2 phase percentages	% of total cells
MTT viability dataset	Supportive endpoint (IC50 determination)	11 concentrations (0–100 µg/mL)	3	Cell viability at each concentration	% of control

Cytotoxic Effects
MTT assay revealed a dose-dependent reduction in PA-1 cell viability following thymoquinone treatment (Table 2, Figure 1). Viability decreased progressively across the concentration range: 90.7% at 10 µg/mL, 81.5% at 20 µg/mL, 75.15% at 30 µg/mL, 72.88% at 40 µg/mL, 59.9% at 50 µg/mL, 57.7% at 60 µg/mL, 55.0% at 70 µg/mL, 49.3% at 80 µg/mL, 42.9% at 90 µg/mL, and 41.8% at 100 µg/mL. The IC50 was estimated at 78.77 µg/mL by linear interpolation between 70 µg/mL (55.0% viability) and 80 µg/mL (49.3% viability).

Table 2: MTT Dose-Response and IC50

Thymoquinone concentration (µg/mL)	Cell viability (% of control)
0	100.0
10	90.7
20	81.5
30	75.15
40	72.88
50	59.9
60	57.7

Thymoquinone concentration (µg/mL)	Cell viability (% of control)
70	55.0
80	49.3
90	42.9
100	41.8
IC50 (estimated by linear interpolation within the tested range)	78.77

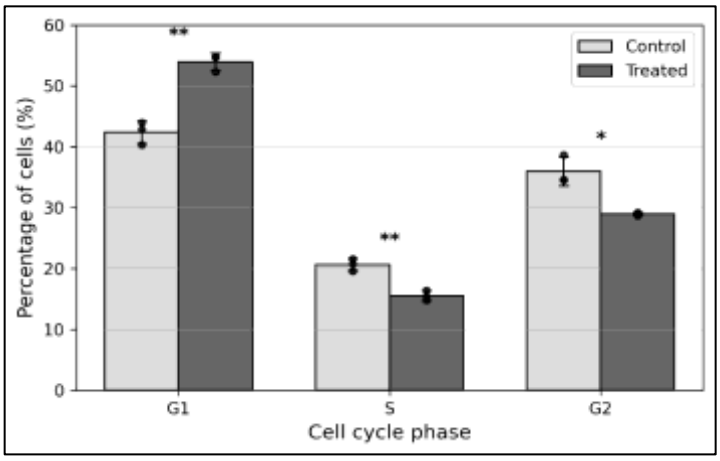

FIGURE 1: MTT Dose-Response Curve

Cell Cycle Redistribution

Flow cytometry analysis revealed alterations in cell cycle distribution following thymoquinone treatment (Table 3, Figure 2).

Table 3: Cell Cycle Statistics

Cell cycle phase	Control (mean ± SD, %)	Treated (mean ± SD, %)	n per group	Welch p	BH-FDR p
G1	42.35 ± 1.88	53.91 ± 1.43	3	0.0014	0.0032
S	20.64 ± 1.00	15.53 ± 0.82	3	0.0028	0.0051
G2	35.93 ± 2.37	28.94 ± 0.27	3	0.0347	0.0425

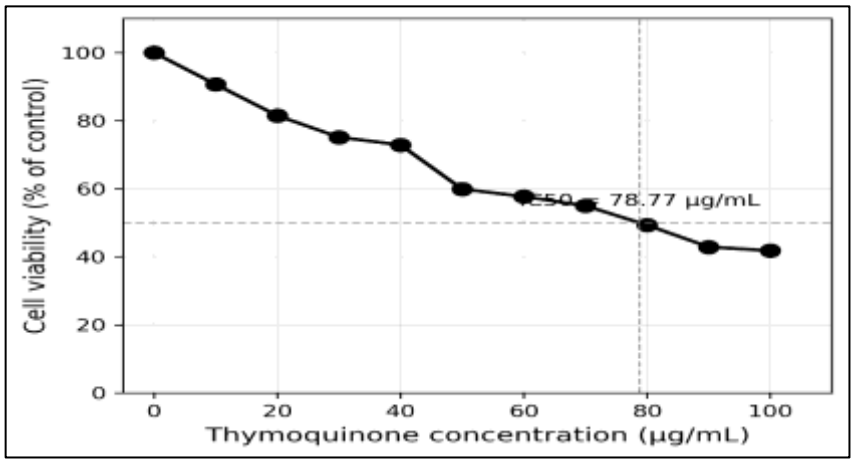

FIGURE 2: Cell Cycle Distribution

The G1 phase showed accumulation in the treated cells. The percentage of G1-phase cells increased from 42.35±1.88% in controls to 53.91±1.43% in treated cells (Welch's t-test, p=0.00144; BH-FDR, p=0.00317), a 27% relative increase. The individual replicate values for control G1 were 43.96%, 40.28%, and 42.82%. The treated replicate values were 54.82%, 54.66%, and 52.26%, respectively

The S phase decreased with treatment. Control cells showed 20.64±1.00% in S phase (replicates: 21.58%, 19.58%, 20.75%), while treated cells showed 15.53±0.82% (replicates: 15.4%, 14.78%, 16.4%). This represented a 25% relative reduction (Welch's p = 0.00278; BH-FDR p = 0.00509).

The G2 phase also decreased following treatment. Control cells distributed 35.93±2.37% in G2 phase (replicates: 34.54%, 38.66%, 34.58%), compared to 28.94±0.27% in treated cells (replicates: 28.66%, 29.2%, 28.96%). This 19% relative reduction was statistically significant (Welch's p = 0.0347; BH-FDR p = 0.0425). Treated cells showed lower variability in G2 distribution (SD 0.27%) than control cells (SD 2.37%).

All three cell cycle phase changes remained statistically significant after the Benjamini-Hochberg FDR correction for multiple testing.

DISCUSSION

G1 phase cells increased by 27% following thymoquinone treatment (Table 3, Figure 2), accompanied by reductions in S-phase (25%) and G2-phase (19%) cells. This redistribution suggests interference at the G1/S checkpoint. The G1/S checkpoint controls entry into DNA synthesis and is regulated by cyclin-dependent kinase (CDK) complexes (15). Breast cancer studies show similar G1 accumulation with p21 upregulation and cyclin D1 downregulation (11, 16). In colon cancer models, thymoquinone treatment has been reported to affect cyclin E-CDK2 complex formation (12, 17). The magnitude of effect in this dataset was comparable to that reported in previous studies.

The concurrent reduction in S and G2 phases indicated reduced progression into DNA synthesis and mitosis. This pattern suggests disruption at the G1/S transition point (18). The consistent effect across technical replicates supports the reproducibility of this finding under the experimental conditions tested.

The IC50 of 78.77 µg/mL falls within the range reported for thymoquinone in other ovarian cancer models (16). Differences in cell lines, exposure duration, and viability assays limit direct comparisons. Viability progressively declined with increasing concentration. At 50 µg/mL, viability decreased to 59.9%, and at 80 µg/mL, it decreased to 49.3%.

The cell cycle and viability data indicated that G1 enrichment contributed to growth inhibition. At higher concentrations, cytotoxicity likely involves mechanisms beyond cell cycle redistribution. Oxidative stress, mitochondrial dysfunction, and apoptosis have been documented in thymoquinone-treated cancer cells (7,8). These measurements do not establish whether G1 accumulation precedes or accompanies other cytotoxicities.

G1 enrichment blocks DNA replication without triggering apoptosis. This may be relevant to combination strategies involving DNA-damaging agents or other cell cycle modulators. The S-phase reduction suggests that thymoquinone effectively prevents entry into the DNA synthesis phase. The translational relevance of these in vitro findings requires careful consideration in future studies. IC50 values provide initial benchmarks but must be evaluated against achievable plasma concentrations and tumor pharmacokinetics.

G1 phase cells increased by 27% following thymoquinone treatment (Table 3, Figure 2), accompanied by reductions in S-phase (25%) and G2-phase (19%) cells. This redistribution suggests interference at the G1/S checkpoint. The G1/S checkpoint controls entry into DNA synthesis and is regulated by cyclin-dependent kinase (CDK) complexes (15). Breast cancer studies show similar G1 accumulation with p21 upregulation and cyclin D1 downregulation (11, 16). In colon cancer models, thymoquinone treatment has been reported to affect cyclin E-CDK2 complex formation (12, 17). The magnitude of effect in this dataset was comparable to that reported in previous studies.

The concurrent reduction in S and G2 phases indicated reduced progression into DNA synthesis and mitosis. This pattern suggests disruption at the G1/S transition point (18). The consistent effect across technical replicates supports the reproducibility of this finding under the experimental conditions tested.

The IC50 of 78.77 µg/mL falls within the range reported for thymoquinone in other ovarian cancer models (16). Differences in cell lines, exposure duration, and viability assays limit direct comparisons. Viability progressively declined with increasing concentration. At 50 µg/mL, viability decreased to 59.9%, and at 80 µg/mL, it decreased to 49.3%.

LIMITATIONS

study had several limitations. First, technical rather than biological replicates were used. Technical replicates demonstrate reproducibility within a single experiment but cannot account for variability between experiments. Technical replicates showed low variability (G1: SD 0.27–1.88%; S: SD 0.82–1.00%; G2: SD 0.27–2.37%), indicating reproducibility despite the absence of biological replicates, which are needed to assess inter-sample variation.

Second, we analyzed only a single treatment condition. Time-course experiments would clarify the kinetics and distinguish between early and late effects.

Third, we studied a single ovarian cancer cell line. PA-1 cells are derived from an ovarian teratocarcinoma and may not fully represent high-grade serous ovarian carcinoma, the most common and lethal subtype. Validation across multiple cell lines with diverse genetic backgrounds would strengthen the generalizability of our findings.

Fourth, flow cytometry quantifies cell cycle distribution at a single time point but does not distinguish between reversible growth arrest and terminal cell cycle exit, which requires long-term tracking studies or clonogenic assays to determine.

CONCLUSION

Thymoquinone treatment was associated with G1-phase accumulation in PA-1 ovarian cancer cells, accompanied by corresponding reductions in the S and G2 phases. The compound exhibited a dose-dependent decrease in viability, with an estimated IC50 of 78.77 µg/mL in this dataset. These findings merit further investigation into cell cycle effects in ovarian cancer models. Future studies should characterize the dose-response relationships for cell cycle effects, validate the findings across diverse ovarian cancer cell lines, examine the molecular basis of G1 accumulation, and investigate the interactions between cell cycle effects and other anticancer mechanisms of thymoquinone.

REFERENCES

1. Krishan A. Rapid flow cytofluorometric analysis of mammalian cell cycle by propidium iodide staining. J Cell Biol. 1975 Apr;66(1):188-93. PMID: 49354.
2. Gerlier D, Thomasset N. Use of MTT colorimetric assay to measure cell activation. J Immunol Methods. 1986 Jul 15;94(1-2):57-63. doi: 10.1016/0022-1759(86)90215-2. PMID: 3782817.
3. Mosmann T. Rapid colorimetric assay for cellular growth and survival: application to proliferation and cytotoxicity assays. J Immunol Methods. 1983 Dec 16;65(1-2):55-63. doi: 10.1016/0022-1759(83)90303-4. PMID: 6606682.
4. Shoieb AM, Elgayyar M, Dudrick PS, Bell JL, Tithof PK. In vitro inhibition of growth and induction of apoptosis in cancer cell lines by thymoquinone. Int J Oncol. 2003 Jan;22(1):107-13. PMID: 12469192.
5. Gali-Muhtasib HU, Kuester D, Mawrin C, et al. Molecular pathway for thymoquinone-induced cell-cycle arrest and apoptosis in neoplastic keratinocytes. Int J Oncol. 2004 Mar;24(3):661-8. PMID: 15057144.
6. Wilson-Simpson F, Vance S, Schwarting R. Physiological responses of ES-2 ovarian cell line following ascorbate treatment and photodynamic therapy. Photochem Photobiol. 2007 Mar-Apr;83(2):397-403. doi: 10.1562/2006-06-21-RA-935. PMID: 17487111.
7. Khan MA, Tania M, Wei C, et al. Molecular targeting of Akt by thymoquinone promotes G1 arrest through translation inhibition of cyclin D1 in breast cancer cells. Life Sci. 2013 Nov 12;93(21):783-90. doi: 10.1016/j.lfs.2013.09.009. PMID: 24044882.
8. Atas E, Gönüllü G, Öztoprak I, et al. How claudin-1 and MMP-2 expression in retinoblastoma affects tumor invasion and metastasis. Turk J Med Sci. 2015;45(4):795-803. doi: 10.3906/sag-1405-125. PMID: 26122225.
9. Al Moundhri MS, Al Abousi SS, Al Mahrouqi RA, et al. Thymoquinone enhances cisplatin-response through direct tumor effects in a syngeneic mouse model of ovarian cancer. J Ovarian Res. 2015 Jul 24;8:38. doi: 10.1186/s13048-015-0177-8. PMID: 26215403.
10. Gao Y, Zhang R, Dai S, et al. Enhanced antitumor efficacy of gemcitabine in combination with metformin in pancreatic cancer. Oncol Lett. 2015 Dec;10(6):3527-3531. doi: 10.3892/ol.2015.3786. PMID: 26552746.
11. Ayob AZ, Mohd Bohari SP, Abd Samad A, Jamil S. Thymoquinone induces apoptosis and increase ROS in ovarian cancer cell line. Cell Mol Biol (Noisy-le-grand). 2016 Jun 30;62(7):97-101. PMID: 27262811.
12. Liu X, Wang Y, Wang R, Li S. The effect of thymoquinone on apoptosis of SK-OV-3 ovarian cancer cells. J BUON. 2017 Nov-Dec;22(6):1455-1461. PMID: 28692636.
13. Al Kusaibi A, Al-Azzawi S, Al Mahrooqi S, et al. Chemopreventive effect of thymoquinone on colon carcinogenesis. Oncol Lett. 2018 Apr;15(4):3810-3819. doi: 10.3892/ol.2018.7805. PMID: 29519737.
14. Li X, Xu H, Wang Y, et al. Thymoquinone inhibits proliferation and induces apoptosis of human renal cell carcinoma cells through the JAK2/STAT3 signaling pathway. Oncol Rep. 2020 Sep;44(3):1194-1204. doi: 10.3892/or.2020.7685. PMID: 32670815.
15. Rashidmayvan M, Rahbar Saadat Y, Hosseiniyan Khatibi SM, et al. Thymoquinone: A novel strategy for cancer treatment. J Cell Physiol. 2021 Aug;236(8):5491-5516. doi: 10.1002/jcp.30244. PMID: 33923474.
16. Dehghani H, Jafary H, Javadzadeh Y, et al. The comparison of anticancer activity of thymoquinone, its solid dispersion and combination with paclitaxel on ovarian cancer cells. Iran J Pharm Res. 2024;23(2):e125355. doi: 10.5812/ijpr-125355. PMID: 39536185.